Back to Session Subjects

A LOW COST APPROACH TO HELICOPTER HEALTH AND USAGE MONITORING

Eric C. Lee[1], Graham F. Forsyth[2], and Cees Bil[3]

[1] RMIT University
506 Lorimer Street Fishermans Bend VIC 3207, Australia
e-mail: Eric.Lee@dsto.defence.gov.au

[2] Defence Science and Technology Organisation, DSTO
506 Lorimer Street Fishermans Bend VIC 3207, Australia
e-mail: Graham.Forsyth@dsto.defence.gov.au

[3] RMIT University
GPO Box 2476V Melbourne VIC 3001, Australia
e-mail: C.Bil@rmit.edu.au

Key words: HUMS, Detection Indices, Helicopter

Abstract: This paper describes a low cost approach to helicopter health and usage monitoring, which could potentially enable smaller size, lower cost, and older helicopters to have similar HUMS (Health and Usage Monitoring System) benefits as to the larger more expansive helicopters. The system prescribed is called 'SmartHUMS', a miniature HUMS unit developed by the Defence Science and Technology Organisation (DSTO) of Australia in cooperation with GPS Online Pty Ltd. The emphasis of this paper is not the hardware aspects of the SmartHUMS unit, but instead on the development of algorithms that can be utilised by the SmartHUMS unit. The algorithms must be generic, simple, and should not require a complicated computational system, but at still maintain high accuracy of health and usage monitoring. The algorithms developed in this research are referred as Detection Indices (DI).

This paper demonstrates the DI capability using a bench top test rig driven by a two-stroke model helicopter motor. Faults were purposely introduced to the rig during its operation. Besides the bench top experiment a flight test experiment performed onboard a Hughes 300 helicopter was also conducted. The helicopter experiment consisted of pilot induced manoeuvre effects. The results of the experiments are presented in this paper.

1 INTRODUCTION

Helicopters have a higher rate of mechanical failure accidents because they are more vulnerable to catastrophic mechanical failures than fixed wing aircraft [1]. The accidents occur simply because of the higher number of single load path critical parts within the rotor and transmission systems and the reduced redundancy within the helicopter design [2]. To decrease the instance rate, equipment capable of detailed monitoring of different critical helicopter functions are routinely fitted to medium-sized and larger helicopters used by civil and some military operators. The combination of these equipment forms a system that is capable of monitoring many different critical parts of a helicopter. This system is usually referred to as Health and Usage Monitoring System (HUMS). The major trigger for the development of HUMS in the UK and Europe is largely due to the recommendation of the CAA-commissioned HARP report in 1984, where the report suggested that HUMS could be retrofitted onto existing rotorcraft and incorporated into new helicopter types [3]. Between 1991 and 1997, CAA studies have shown HUMS were able to provide warnings for 69% of the failure types and successfully warned 60% of all the potentially catastrophic failure cases.

Currently, vibration health monitoring systems have been made mandatory in the UK on large helicopters certified or validated since certification requirements were tightened by the CAA after the HARP report. An additional airworthiness directive in 1999 also made vibration health monitoring systems mandatory in the UK on older types of helicopter carrying more than 9 passengers [3]. The main reason why only large helicopters are being fitted with HUMS is mainly due to the cost issue. Larger helicopters generally cost a lot more, and to make matter worse a capable HUMS usually cost quite considerably. Most helicopter operators consider installing HUMS in their fleet only if the system would provide significant economic benefits that would outweigh the costs in the short term. As majority benefits of HUMS implementation is distributed over the remaining life of the aircraft, which is why older types of helicopter are less likely to be considered for HUMS implementation.

Another reason why HUMS are rarely considered for smaller helicopters is to do with its physical size. In a small helicopter the payload dimension and weight are critical factors. Unfortunately HUMS generally have noticeable size and weight, as well as being generally too expensive to be justified to be fitted in a platform that might cost less. Therefore, this paper introduces a possible solution, which will allow some of the HUMS benefits to be achieved in small and medium sized helicopter. The solution is a low cost light weight miniature 'SmartHUMS' unit combined with the proposed DI algorithms.

The way the proposed DI algorithms work is that during the monitoring process the DI will continuously examine the vibration signal produced by a helicopter. If an adverse condition develops DI will flag the event and only record the vibration data corresponding to the event for further analysis. The event recorded is not necessarily fault induced. The event could just be an abrupt control input by the pilot (i.e. aircraft manoeuvre). This is where the proposed DI differs from conventional HUMS. While conventional HUMS use algorithms that specifically look for individual faults (or faults in individual gears, bearings, etc.), the DI techniques looks for events in terms of changes in transfer functions. For example, a conventional HUMS only detect a structural crack if an algorithm to detect cracks is included, while SmartHUMS would detect the crack as long as it affects the transfer of any significant signal. This low cost HUMS approach is not able and capable of replacing existing HUMS, but in the contrary the combination of a SmartHUMS unit and selected DI aims to extend or assist current HUMS technology and to apply HUMS benefits into areas which were previously thought to be financially impossible or physically impractical to be applied.

2 PROPOSED DI

The two selected DI algorithms investigated in this paper are: Autocorrelation (sometimes called serial correlation) and Cross-Correlation.

2.1 Autocorrelation

According to [4], time series data sometimes show repetitive behaviour or other properties where current values have some relation to the earlier values. Autocorrelation is a statistic that measures the degree of this affiliation. The ability of autocorrelation to determine changes to otherwise regular patterns sets an excellent backdrop for the DI application. If, during the monitoring of a mechanical vehicle, a difference is detected between the behaviour of the current data from that relating to the previous period, the raw data during both period is stored and compressed for further analysis. The autocorrelation technique has two most significant parameters, which are the time series data length and the lag amount. Essentially the lag amount is the parameter that allows the comparison of the time series to itself. If the lag amount is equal to 1, the time series data is being compared to itself shifted by one data point at a time.

The other advantage of using autocorrelation as a DI is that it has the capacity of detecting periodic patterns even in the presence of random data (noise). If the time series contain large amount of noise, the autocorrelation process will still be able to present the periodic patterns by filtering out most of the noise.

The general mathematical expression for autocorrelation function is commonly described as [5, 6]:

$$R_x(\tau) = \lim_{T \to \infty} \frac{1}{T} \int_0^T x(t)x(t+\tau)dt \qquad (1)$$

Where T is the record length, Rx(τ) represents the value of the autocorrelation function at the time delay τ, x(t) represents the value of the signal x at time t, and x(t+τ) is the value of the signal x at delayed time t+τ. In terms of discrete time, Eq. 1 becomes:

$$R_m = \frac{1}{N\text{-}m} \sum_{t=1}^{N\text{-}m} (x_t)(x_{t+m}) \approx \frac{1}{N} \sum_{t=1}^{N\text{-}m} (x_t)(x_{t+m}) \qquad (2)$$

Where N (sample size) is the approximation of N-m (the difference between N-m and N is in fact negligible in most cases), and m is the delay value called lag. Introducing x,¯ (mean of entire time series) into Eq. 2 gives:

$$Autocovariance = \frac{1}{N} \sum_{t=1}^{N\text{-}m} (x_t - \bar{x})(x_{t+m} - \bar{x}) \qquad (3)$$

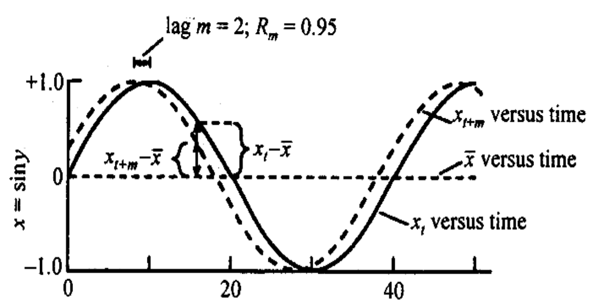

Figure 1: Time series (solid), lags (dashed) [4]

Autocovariance is one of the two major components in the formulation of the autocorrelation coefficient function for a given lag value. According to [4], autocovariance literally means, “How something varies with itself”, where a time series gets compared to itself and the main tool in the system is the lag. It is a quick way of evaluating deviations between the one unaltered time series and one that is lagged, as shown in Fig. 1. When generating autocovariance there are two rules of thumb [7]. The first rule is that the data set should contain more than 50 values. The second rule is the largest lag for the autocovariance calculation is equal to one quarter of the total number of values in the data set.

The second ingredient for the autocorrelation coefficient for a given lag is called variance and it is obtained by standardising Eq. 3 the autocovariance equation, therefore it can then be compared directly to other standardised autocovariances [4]. The equation for variance is basically the sum of the square term $(x_t-\bar{x})^2$ for each observation in the original time series, divided by N:

$$Variance = \frac{1}{N}\sum_{t=1}^{N}(x_t-\bar{x})^2 \tag{4}$$

With the equation for both components known, the description for the autocorrelation coefficient for a given lag is basically the autocovariance divided by the variance as presented in Eq. 5:

$$\text{Autocorrelation } (R_m) = \frac{\text{autocovariance}}{\text{variance}}$$

$$= \frac{\frac{1}{N}\sum_{t=1}^{N-m}(x_t-\bar{x})(x_{t+m}-\bar{x})}{\frac{1}{N}\sum_{t=1}^{N}(x_t-\bar{x})^2} = \frac{\sum_{t=1}^{N-m}(x_t-\bar{x})(x_{t+m}-\bar{x})}{\sum_{t=1}^{N}(x_t-\bar{x})^2} \tag{5}$$

Eq. 5 is one of the many forms that describe the autocorrelation coefficient approximation, also called the lag autocorrelation coefficient or the lag serial correlation coefficient. The autocorrelation coefficient values range between +1 to –1, with +1 meaning the time series compared are exact duplicates of each other, which also means the lag value is equal to zero, and –1 meaning the time series compared are mirror images of each other. Zero means the compared time series have no relation to each other, which basically means they are random.

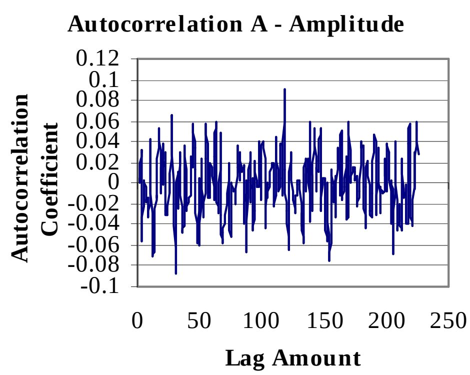

Figure 2: Uncorrelated Correlogram (random)

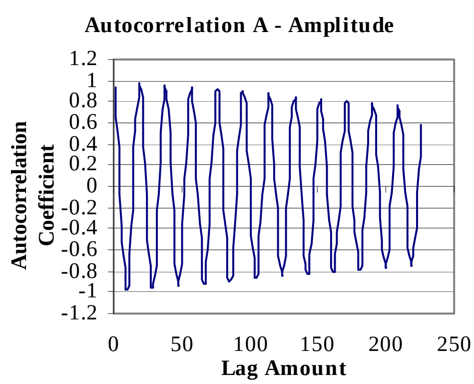

Figure 3: Correlated Correlogram

A common way of analysing the autocorrelation coefficients and their respective lag values is by plotting the autocorrelation coefficient against the lags. The plot is called a correlogram and is a comprehensive way to indicate the relationship between time series data. In the case where the time series have no relationship to each other, the correlogram will present an irregular pattern with amplitude close to zero, except when the lag is equal to zero, as shown in Fig. 2. In contrast, when the time series have a strong relationship, the correlogram will show high coefficient values and a regular pattern as shown in Fig. 3.

2.2 Cross-Correlation

The cross correlation algorithm is a measure of the similarities and shared properties between data series. The arithmetic aspect of cross correlation is very similar to that of the autocorrelation. The only difference is the variable composition. In autocorrelation there is only one series to deal with, but in cross correlation there are usually two data series. The two data series can be any type of series for example related, non-related, or even identical (in such a case, it becomes an autocorrelation analysis). Once the cross correlation has been performed the association between the two data series will be revealed. Similar to the autocorrelation, the cross correlation results are often being described as a non-dimensional format. With the non-dimensional property, it is easier to compare the cross correlated results to other results obtained from different data sources. The non-dimensional cross correlation result is also known as the cross correlation coefficient. Like autocorrelation coefficients, the cross correlation coefficient values always lie between -1 and +1. +1 means 100% correlation in the same sense as autocorrelation analysis, -1 means 100% correlation in the reverse order (anti-phase), and 0 signifies zero correlation (means the series are completely independent of each other) or two completely randomised series.

The application of this DI is to assess the amount of the similarities between two autocorrelated data series, and use this information to decide whether a characteristic change has occurred for the platform in question.

Cross correlation is also a type of statistical analysis. The common mathematical expression for the continuous time cross correlation function is generally defined as [8, 9]:

$$R_{xy}(\tau) = \lim_{T\to\infty} \frac{1}{2T} \int_{-T}^{T} x(t)y(t+\tau)dt \qquad (6)$$

As cross correlation is used to examine the common properties between two sequences of data series, it is required to move the sequences past one another entirely. This prerequisite is different from that of the autocorrelation, where the calculation only compute positive lags from 0 to +T to obtain all possible comparisons between the time series and itself. In the case of cross correlation if two different series are being considered as shown in Eq. 6, the negative lags of the correlation must be considered as well (i.e. incorporated all data from –T to +T). This process will ensure the entire length of one series to move pass the other series, hence all possible match positions are being scrutinised. From Eq. 6, $R_{xy}(\tau)$ represents the value of the cross correlation function at the time delay (or lag) τ, x(t) represents the value of the series x at time t, and $y(t+\tau)$ is the value of the series y at lagged time $t+\tau$.

During the cross correlation analysis, if two data series are identical, the analysis procedure actually becomes very similar to that of autocorrelation analysis. The corresponding results in a cross correlation plot (i.e. cross correlogram) will be a mirror image of itself around lag 0, and with the highest amplitude (i.e. value of 1) at this point. The interpretation of the result in this situation should not be treated as the same as in the autocorrelation. Because in cross correlation one sequence is being ‘moved past’ the other rather than being lagged behind from a position of initial equivalence, it is therefore common to describe the successive comparisons as matched positions rather than lags.

Since the data series examined by the cross correlation are usually in discrete time domain, it is therefore much more convenient to describe Eq. 6 in discrete time as well. The discrete time domain expression for Eq. 6 is very similar to the discrete time domain of the autocorrelation function. The expression is shown in Eq. 7.

$$R_{xy}(m) = \frac{1}{N-m} \sum_{i} (x_i)(y_{i+m}) \approx \frac{1}{N} \sum_{i} (x_i)(y_{i+m}) \qquad (7)$$

N is the series size which is also the approximation of N-m (the difference between N-m and N is in fact small and can be ignore), and m similar to the application of lag value in autocorrelation analysis, but in cross correlation, it is referred to as match position. In the summation term, the variable i is the representation of the time limit –T and +T, as mentioned in order to compare all possible position of the two series, cross correlation computation will started with the negative lags (the match positions that are less than zero or in the negative region) during the analysis.

$$r_{xy}(m) = \frac{\mathrm{CrossCorrelationFunction}}{S_1 \cdot S_2}$$

$$= \frac{\frac{1}{N}\sum_i (x_i - \bar{x})(y_{i+m} - \bar{y})}{\frac{1}{N}\cdot\sqrt{\sum_i (x_i - \bar{x})^2}\cdot\frac{1}{N}\sqrt{\sum_i (y_{i+m} - \bar{y})^2}} = \frac{\sum_i (x_i - \bar{x})(y_{i+m} - \bar{y})}{\sqrt{\sum_i (x_i - \bar{x})^2}\cdot\sqrt{\sum_i (y_{i+m} - \bar{y})^2}} \tag{8}$$

In order to allow the cross correlation solutions to be able to evaluate with other cross correlation results, cross correlation function in Eq. 7 needs to be normalised. The normalisation of Eq. 7 produced the cross correlation coefficient equation which is as shown in Eq. 8. Different to the autocorrelation standardisation procedure, in cross correlation the standardisation is done using the standard deviation ($S_{1,}$ S_2) from both compared autocorrelated data sources as shown in Eq. 8. Also different to the autocorrelation standardisation procedure, the cross correlation mean values ($x,^{-}$, $y,^{-}$) of both data sources are included in the equation to minimise the data calibration requirement for the comparison purposes.

Similar to the autocorrelation DI the easiest way to understand the characteristics of cross correlation coefficients is to plot them. The cross correlation coefficient plot is usually referred to as ‘Cross Correlogram’, which has the same amplitude range between +1 and -1 as the correlogram from autocorrelation. However, with the cross correlogram the horizontal axis contain parameters which are match positions rather than lag values. If the majority of the match positions shown high amplitude of coefficient and the cross correlogram shows high degree of organised cyclic patterns, which basically means the two compared autocorrelated data series have high correlation to each other.

High correlation in cross correlation analysis actually means both series shared large numbers of common properties and characteristics. If the maximum cross coefficient amplitude of 1 (in an ideal case) is achieved at the match position 0, and couple with both cross correlogram from – and + region are mirror image of each other. The two autocorrelated series in this case are very likely to be identical. In real life, however, cases of minor discrepancies for the properties mentioned are always to be expected. Fig. 4 contains a cross correlogram representing the cross correlation analysis of two identical (ideal case) autocorrelated data series. Fig. 5 presents the superimposed plot of – region and + region of the cross correlogram of Fig. 4. As the plot shown in Fig. 5, the – and + region of the plot is exactly identical, which means they are mirror image of one another.

In the case where two autocorrelated data series have no relation or shared properties (i.e. random) with each other, the corresponding cross correlogram plot is presented in Fig. 6, where the amplitudes of the plot are almost equal to zero. Most importantly, the maximum amplitude does not occur at match position 0.

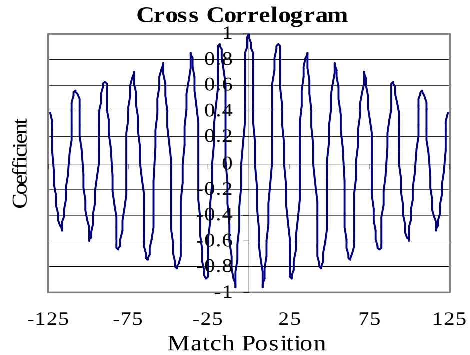

Figure 4: Highly correlated cross correlogram

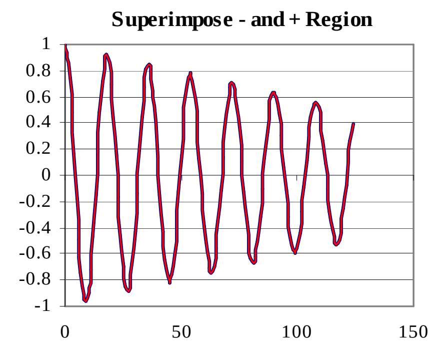

Figure 5: Superimposed plot of Fig. 4

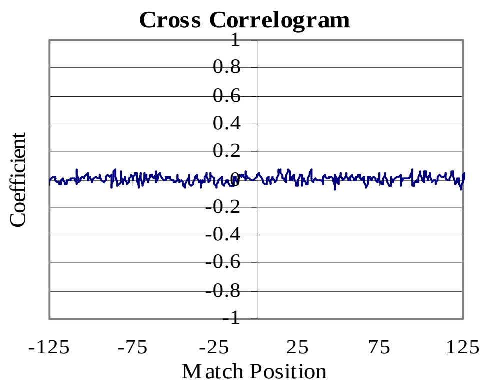

Figure 6: Uncorrelated cross correlogram

3 EXPERIMENTS

Two different experiments were performed to verify the capability of the proposed DI to detect system behavioural change. The first experiment conduced is a test rig setup that consist of a two-stroke model helicopter engine and a two-bladed propeller. The second experiment is a real helicopter (Hughes 300) flight trial experiment. The main purpose of conducting test rig experiment is because for the helicopter flight experiment real fault cannot be introduced. As a result, the test rig setup was utilised to demonstrate real fault detection using the selected DI algorithms.

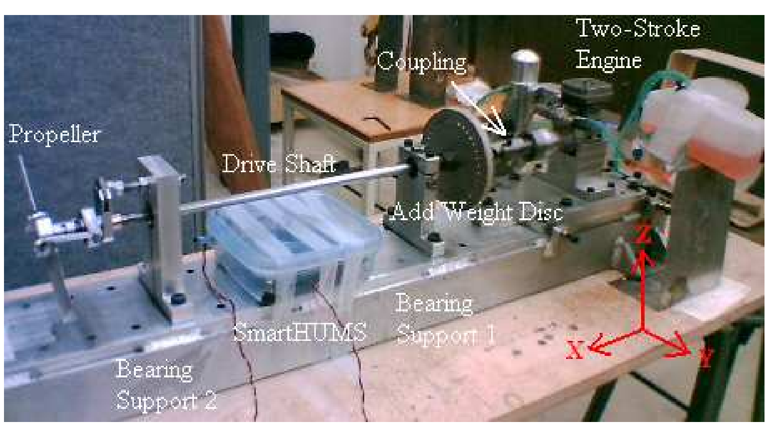

Figure 7: Two-stroke motor test rig

3.1 Two-Stroke Motor Test Rig Experiment

Fig. 7 is the figure showing the actual test setup arrangement of the two-stroke motor test rig. In order to produce a genuine fault situation it was decided to simulate a loose bolt condition in one of the bearing housing base mounts. The base of the bearing housing is actually bolted down by two bolts, and the intention is to loose one of the bolts sometime during the operation of the test rig, and to see whether the DI algorithms will be able to detect the loosening effect of the bearing housing. The bearing housing and its mounting points are shown in Fig. 8, where bolt 2 is the bolt that was loosed during the experiment. The actual procedure during the experiment was after 10^{th} second of the experiment bolt 2 was set to loose and after 20^{th} second bolt 2 was retighten. Therefore, two behavioral change events should be detected for this experiment one is the loose of bolt 2 and the other one is the retightening of the bolt 2.

Figure 8: Bearing housing and its base mount

Fig. 9 presents the autocorrelation and cross correlation correlogram comparisons for 9^{th}, 10^{th} and 11^{th} second of Z-axis experimental data. The main reason why only Z-axis data is being analysed is because bolt 1 and bolt 2 are fixed in vertical (Z-axis) direction. The autocorrelation correlogram comparison between 9^{th} and 10^{th} second of the experimental data indicated that both plots generally overlapped quite well except some amplitude variations. In autocorrelation correlogram comparison amplitude variations generally signify random interferences. The cross correlogram plot for 9^{th} and 10^{th} second experimental data shows high correlation coefficient values, especially the maximum coefficient occurred at match position 0. When maximum coefficient occurred at match position 0, the two cross correlated data sets are highly correlated to each other. The cross correlogram plot for 9^{th} and 10^{th} second also indicated that one side of the correlogram has slightly higher amplitude than the other, which is a characteristic usually associated with speed variation.

Fig. 10 is a zoom in plot of autocorrelation correlogram comparison between 9^{th} second and 10^{th} second of the experiment. From Fig. 10 it is clear the phase alignment is starting to get offset after lag value 150, which proves the speculation of speed variation. During the two-stroke test rig experiment it was found the engine did not always stay in constant rotation, gradual speed variations were occasionally observed. With the random effects and minor inconsistent operation of the two-stroke engine, it is logical to assume there was no significant system behavioural change detected between 9^{th} and 10^{th} second of the experiment. Same observation cannot be said for comparison between 10^{th} and 11^{th} second of the experiment. As shown in lower half of Fig. 9 both autocorrelation and cross correlation correlograms show the compared data sets are clearly very different. The autocorrelation comparison shows no commonality between 10^{th} and 11^{th} second of the experimental data, as well as, the cross correlogram plot only evolved around the zero horizontal axis (almost becomes pure random). As a result, significant system behavioural change has been detected. As described before the bolt 2 was loosed after 10th second of the experiment, therefore, the DI has managed to detect the loosening effect of the bearing housing.

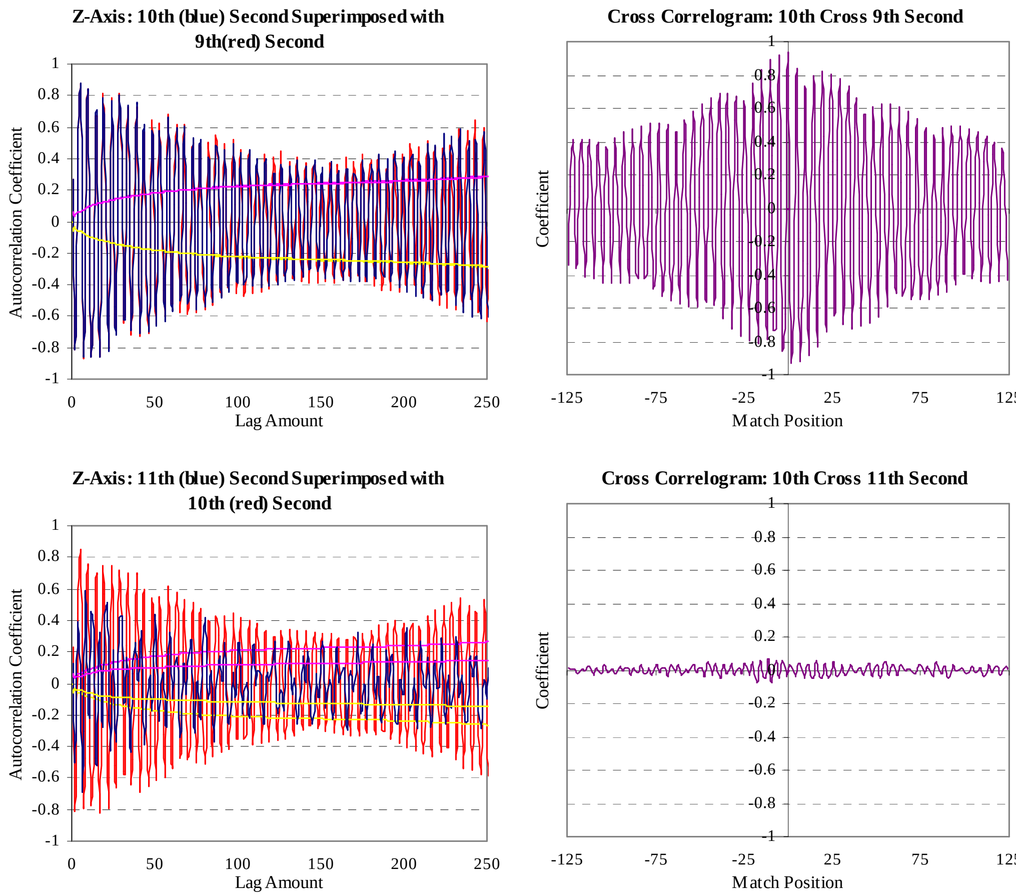

Figure 9: Autocorrelation and cross correlation correlogram comparisons for 9th, 10th, and 11th second of the two-stroke test rig experiment

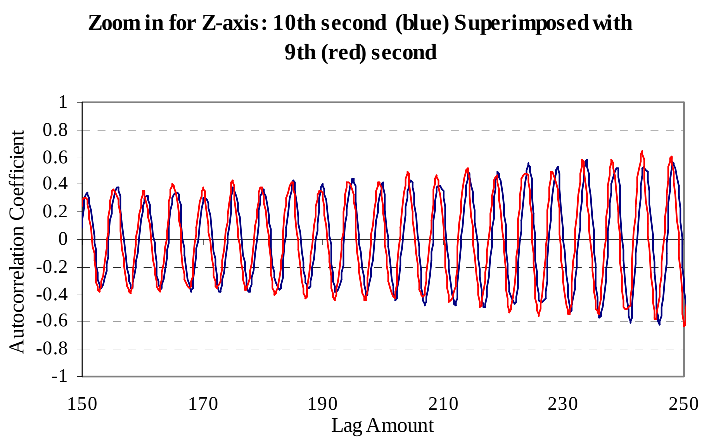

Figure 10: Zoom in plot between lag value 150 and 250

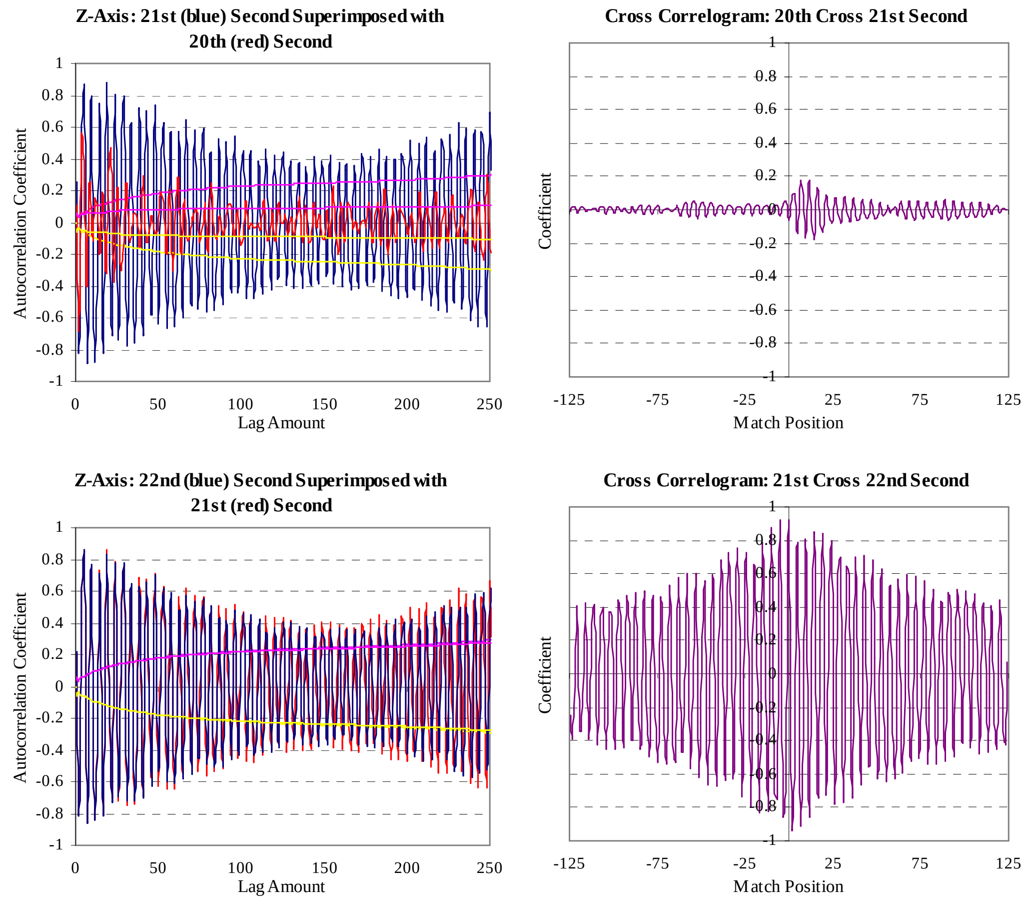

Figure 11: Autocorrelation and cross correlation correlogram comparisons for 20th, 21st, and 22nd second of the two-stroke test rig experiment

Fig. 11 presents the autocorrelation and cross correlation correlogram comparisons for 20th, 21st and 22nd second of the experimental data. Quite obviously from Fig. 11 the autocorrelation correlogram comparison and corresponding cross correlation correlogram for 20th second and 21st second of the experimental data shows significant system behavioural change. The autocorrelation correlogram of 20th and 21st second are very different, which can be further proved by referring to the cross correlogram where the plot has very low amplitude values and basically collapsed around the zero horizontal axis (random). Since bolt 2 was retighten around 20th second of the experiment, the DI managed to pickup the retightening procedure performed. Similar to the explanation for the comparison between 9th second and 10th second of the experimental data, the comparison results observed for 21st and 22nd second data at lower half of Fig. 11 are assumed to contain no significant system behavioural change. Therefore, after bolt 2 was retightened the test rig went back to its steady state of operation.

Fig. 12 is a frequency domain plot of experimental data recorded during 14th second of the test rig experiment. At 14th second the bolt 2 was still loose, hence the plot represents fault condition existed within the test rig system. The fundamental peak observed from Fig. 12 actually represents the operational speed of the test rig during the experiment. The operational speed during the experiment was around 100 Hz. A small red coloured rectangular box can be also observed in Fig. 12, this box actually highlights a lower spectrum peak just before the fundamental that represents the rotational speed. From machine dynamic analogy this phenomenon usually occurs when a bearing is loose on the drive shaft [10]. Since the 14th second data represents bearing housing loose condition and because the bearing is rigidly contained within the housing, as the bearing housing trembles the bearing inside will therefore also vibrate on the drive shaft. Consequently the 'bearing loose on drive shaft' characteristic is being detected. The purpose of DI is to enable the SmartHUMS unit to isolate vital data (data contain system behavioural change) during the monitoring process, and to interpret these data in order to give a general idea of what is likely the cause of this system characteristic change. As the vital data are recorded and probable cause of system behavioural change is being identified (i.e. gear problem), then method developed by other researchers (i.e. A Model-Based Gear Diagnostic Technique [11]) that specifically designed to analyse particular mechanical fault can be applied to further examine the severity and actual location of the fault.

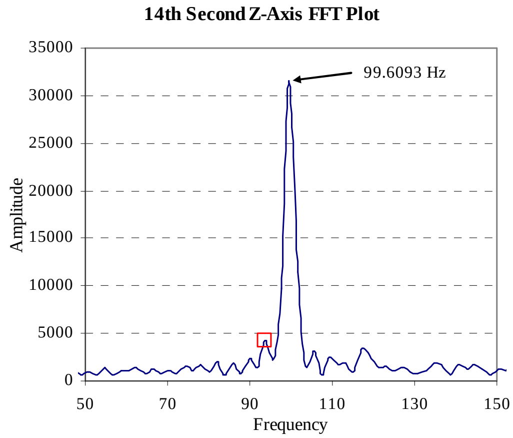

Figure 12: Frequency analysis result for 14th second of the test rig experiment

3.2 Hughes 300 Helicopter Flight Experiment

The idea of the helicopter flight trial experiment is to test whether the selected DI algorithms will work as intended in a real life condition. Fig. 13 is the photo of the Hughes 300 helicopter used for the flight experiment. As the helicopter can only seated two occupants it is considered as a small size helicopter. During the experiment no mechanical related fault was introduced due to OH&S issue (Occupational Health and Safety issues). As a result, only severe manoeuvres (large movements to all controls) were introduced at a noted time after reaching a stable cruise condition. Fig. 14 shows the cross correlation results of flight experiment from 13th second to 16th second.

Figure 13: Hughes 300 helicopter

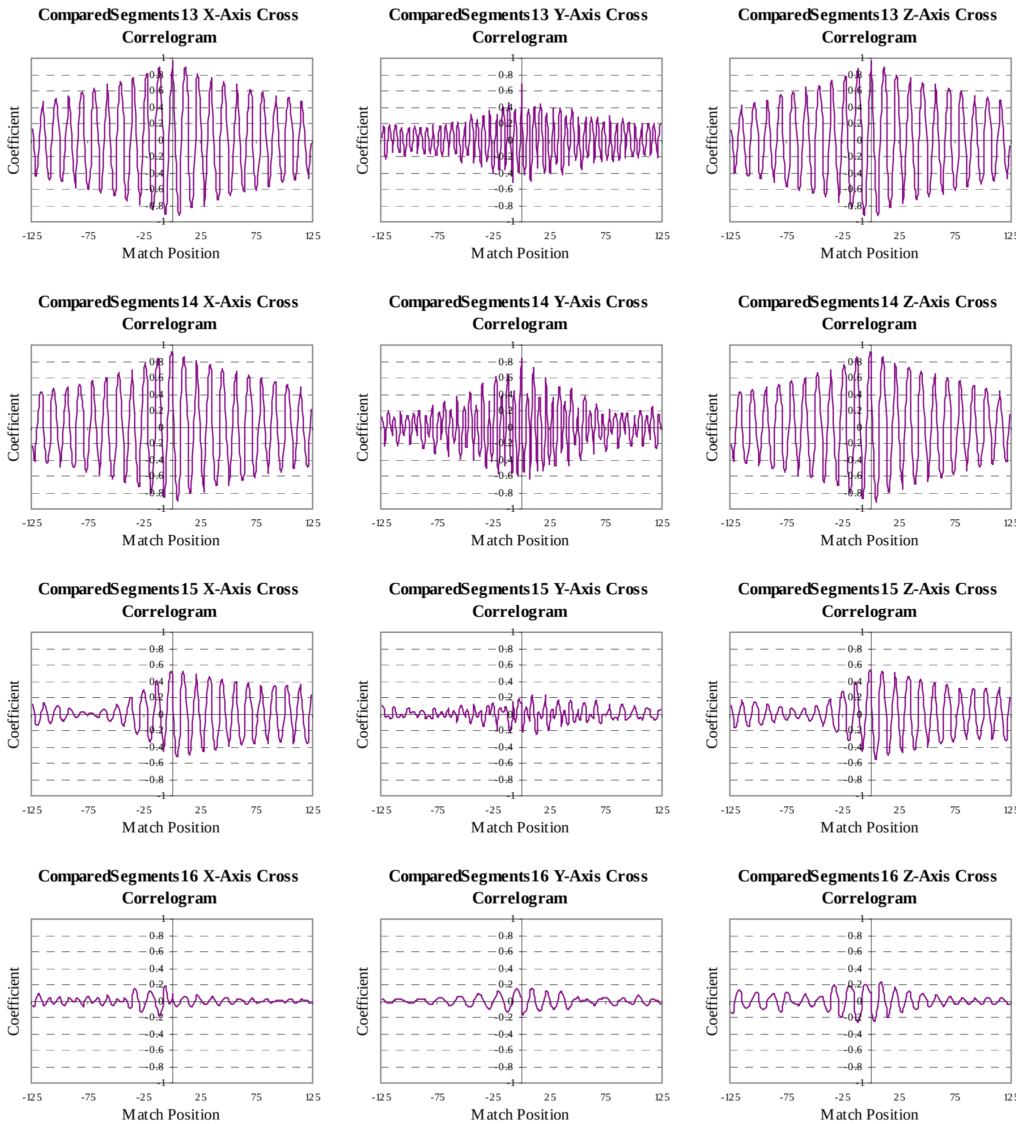

Figure 14: XYZ axes cross correlogram from 13th second to 16th second of flight trial

From Fig. 14 it is quite noticeable that the XYZ axes cross correlogram plots become significantly less correlated (extensive reduction of coefficient values) from 14th second to 15th second of the flight trial experiment. Certain portion of X and Z axes cross correlogram plot patterns for 15th second flight data almost collapse around the zero horizontal axis (random characteristic). As for the Y-axis 15th second cross correlogram plot the patterns are disorganised as well as evolved around the zero horizontal axis (random). Fig. 15 shows the XYZ axes autocorrelation comparison result between flight data 14th second and 15th second. From Fig. 15 is it quite clear that Y-axis comparison plot consists of low coefficients and less organised plot patterns. As the flight condition was in a cruise flight state, majority of forces were in forward (X-axis) and vertical (Z-axis) directions, which is why Y-axis indicates less correlated characteristics. From both X-axis and Y-axis autocorrelation comparison plots the blue correlogram started to become misaligned with the red correlogram from lag value around 150 onwards. The offset of correlogram phases means system behaviour change has occurred. With the cross correlogram results in Fig. 14 and autocorrelation results in Fig. 15, the DI have detected the severe manoeuvres of the helicopter, which was introduced during the 15th second of the flight experiment.

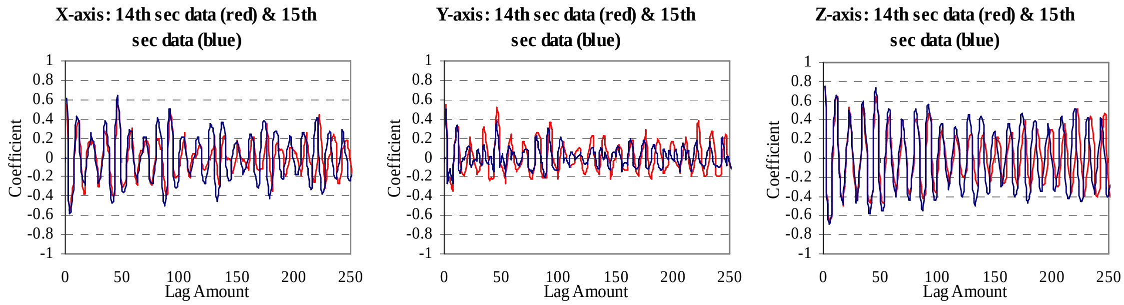

Figure 15: XYZ axes autocorrelation correlogram comparison for 14th and 15th second of flight trial

4 CONCLUSION

Two different experimental test results have been demonstrated in this paper. The purpose of the experiments is to show that selected DI algorithms could be potentially imbedded into a low cost and small physical size HUMS unit called SmartHUMS. The first experiment employed was a two-stroke model engine driven test rig, where the DI were able to detect the loosening characteristic of the bearing housing as well as the retightening action of the bolt 2. With established machine dynamic knowledge the bearing housing looseness was determined through the detection of loose bearing. Since the second experiment involved an actual helicopter, safety (OH&S) issues prevented the use of actual mechanical faults during the helicopter flight, but purposely introduced severe manoeuvres were applied instead. Once again the DI algorithms were able to detect the extreme manoeuvre actions as they appeared. The concept of this low cost SmartHUMS approach might not generate solutions that are as explicit as higher cost and more capable HUMS units, but it is aiming at retaining all important data and giving a general idea of what is the likely cause of system behavioural change. As the essential data are retained further analyses using other researcher's method could be employed to confirm and isolate the actual location of the fault or faults.

5 REFERENCES

[1] Forsyth, G. F., "Workshop on Helicopter Health and Usage Monitoring Systems", DSTO-GD-0197, DSTO, Melbourne Australia, 1999.

[2] Evans, A. J., "Managing a Successful HUMS Operation", Third International Conference on Health and Usage Monitoring – HUMS2003, 2003, pp. 101-124.

[3] CAA, "What is HUMS, and what are its benefits', http://www.caa.co.uk/docs/389/srg_acp_00014-01-300103.pdf

[4] Williams, G. P., "Chaos Theory Tamed", London, Taylor & Francis, 1997.

[5] James, E. B. and Robinson, C., "Description of peak value and illustration of its wide array of applications in fault detection and problem severity assessment", Emerson Process Management Reliability Conference, 2001.

[6] Zubaydi, H. A. and Swamidas, A. S. J., "On the use of the autocorrelation function to identify the damage in the side shell of a ship's hull", Marine Structures, Vol. 13, 2000, pp. 537-551.

[7] Davis, J. C., "Statistics and data analysis in geology", New York, Wiley, 1986.

[8] Miller, M. J., “An introduction to linear channel ‘Identification’ techniques”, South Australian Institute of Technology.
[9] McRae, K. I. and Black, M., “Application of cross correlation to background noise reduction during in-flight acoustic emission monitoring of aircraft structures”, Research and Development Branch Department of National Defence Canada, 1982.
[10] Taylor, J. I., “The Vibration Analysis Handbook”, 1st ed., Tampa FL: Vibration Consultants Inc, 1994.
[11] Wang, W. and Wong, A. K., “A Model-Based Gear Diagnostic Technique”, Defence Science & Technology Organisation Australia, 2000.